

GEOLOGICAL SURVEY CIRCULAR 397



DISCHARGE CHARACTERISTICS  
OF BROAD-CRESTED WEIRS

UNITED STATES DEPARTMENT OF THE INTERIOR  
Fred A. Seaton, *Secretary*

GEOLOGICAL SURVEY  
Thomas B. Nolan, *Director*

---

GEOLOGICAL SURVEY CIRCULAR 397

---

## DISCHARGE CHARACTERISTICS OF BROAD-CRESTED WEIRS

By H. J. Tracy

Washington, D. C., 1957

---

Free on application to the Geological Survey, Washington 25, D. C.

## SYMBOLS

$b$  = weir width, in feet, normal to the direction of flow; also, width of contracted opening

$B$  = width, in feet, of rectangular channel

$C$  = coefficient of discharge

$F$  = Froude number,  $V / \sqrt{gh}$

$g$  = acceleration of gravity

$h$  = height of water surface, in feet, above the crest of the weir measured at a section just upstream from the beginning of acceleration of the fluid as it approaches the weir

$H$  = energy head, in feet,  $h + V_0^2 / 2g$ , where  $V_0$  is the mean velocity of the fluid at the section of approach

$k$  = mean height of boundary-roughness projections, in feet, above the nominal level

$L$  = weir length, in feet, parallel to the direction of flow

$P$  = height of weir, in feet

$q$  = discharge per foot of width

$Q$  = discharge, in cubic feet per second

$r$  = radius of rounding, in feet, at upstream crest

$R$  = Reynolds number,  $Vh\rho/\mu$

$t$  = height of the water surface, in feet, above the crest of the weir, at a section just downstream from the point where the flow has reestablished its normal regime after passing over the weir

$V$  = velocity of flow, in feet per second

$W$  = Weber number,  $V / \sqrt{\sigma / \rho h}$

$y$  = depth of water on weir crest

$\gamma$  = specific weight

$\rho$  = mass density

$\mu$  = viscosity

$\sigma$  = surface tension

# DISCHARGE CHARACTERISTICS OF BROAD-CRESTED WEIRS

By H. J. Tracy

## CONTENTS

	Page		Page
Symbols .....	Faces 1	Weir height .....	7
Abstract .....	1	Nappe form .....	7
Introduction .....	2	Reynolds number .....	8
Control section .....	2	Rounded weir entrance .....	9
Dimensional analysis .....	2	Boundary roughness .....	10
External flow pattern .....	4	Shape ratio .....	11
Discharge coefficient .....	6	Sloping upstream and downstream faces .....	11
Definition .....	6	Submergence .....	11
Effect of parameters influencing the coefficient .....	6	Bibliography .....	15
Weir length .....	6	Published reports .....	15
		Unpublished reports .....	15

## ILLUSTRATIONS

		Page
Figure 1.	Definition sketches of broad-crested weirs with vertical faces and horizontal crest .....	3
2.	Dimensionless water-surface profiles for broad-crested weirs with vertical faces and horizontal crest .....	5
3.	Discharge coefficients for broad-crested weirs with vertical faces and horizontal crest, square entrance .....	6
4.	Effect of the wetted-underneath nappe form on the discharge coefficient .....	7
5.	Effect of the depressed nappe form on the discharge coefficient .....	8
6.	Effect of the detached nappe form on the discharge coefficient .....	9
7.	Variation of the discharge coefficient with scale of weir .....	10
8.	Discharge coefficients for broad-crested weirs with vertical upstream face .....	11
9.	Discharge coefficients for broad-crested weirs with upstream-face slope of 1/2:1 .....	12
10.	Discharge coefficients for broad-crested weirs with upstream-face slope of 1:1 .....	13
11.	Discharge coefficients for broad-crested weirs with upstream-face slope of 2:1 .....	14

## ABSTRACT

Discharge characteristics of broad-crested weirs defined by laboratory tests are described. Broad-crested weirs are classified as short, normal, or long according to the form of the water-surface profile over the weir. The discharge equation is obtained by dimensional analysis, and the coefficient of dis-

charge is related to dimensionless ratios that describe the geometry of the channel and the relative influence of the forces that determine the flow pattern. The effect of these various ratios on the discharge coefficient is shown by the use of existing laboratory data. No new experimental work is involved.

## INTRODUCTION

Frequently, so-called indirect methods of discharge measurement are the only practicable means of obtaining the magnitude of a peak flood flow past a given site. These determinations are based on the water-surface profile, usually defined from high-water marks, and upon the geometry and hydraulic characteristics of the channel. If a transition structure, such as a dam or abrupt channel constriction, is used as the measuring device, the geometry of the structure also affects the water-surface profile for a given discharge. For this reason, a knowledge of the head-discharge relation for a given weir or spillway may prove invaluable for the determination of an important flood peak which could not be otherwise measured.

A flow determination involving a weir or spillway is classified as indirect if the structure is uncalibrated, and the head-discharge relation must be obtained from a comparison with other similar calibrated weirs. Needless to say, the number of possible weir forms is almost unlimited.

This report deals only with the broad-crested weir form. Definition sketches of this weir are shown in figure 1. This study is based on existing data on flow over broad-crested weirs, and no new experimental work is involved. It has not been possible to answer many questions which arise. For example, sufficient data have not been published to define the effect of angularity of crest to direction of flow, of gates and piers, of end abutments, and so on. The question of submergence has also been considered in only a very general manner.

The term "broad-crested weir" is generally poorly defined; usually, this weir has been classified only with respect to the geometry of the structure itself. Almost universally, a weir is called broad-crested if it has a more or less horizontal crest of finite length in the direction of flow. This definition is not entirely adequate, because at sufficiently high head-to-length ratios the nappe tends to spring clear of the weir crest, and the structure no longer performs as a broad-crested weir. At the opposite extreme, for very small head-to-length ratios, the weir crest becomes a reach of open channel in which frictional resistance predominates, and for which the discharge is more properly evaluated by one of the open-channel flow formulas than by a weir formula. It is thus clear that any definition of a broad-crested weir must include the head acting on the weir. This is considered in some detail on page 4.

## CONTROL SECTION

For broad-crested weirs it is usually assumed that the flow will be critical on the weir crest. Traditionally, the weir discharge is determinable from a single depth measurement on the weir crest and the equation

$$q = \sqrt{g} y^{3/2}. \quad (1)$$

This elementary method, however, is not satisfactory when an accurate discharge determination is required. The flow depth does not correspond to that given by equation 1 everywhere on the weir crest. The location of the control, or critical depth, section, is not constant, but varies with discharge, weir geometry, and crest roughness.

The inlet geometry is of primary importance in the location of the critical-flow section. If the weir entrance is not rounded, separation will occur just down-

stream from the entrance, and the critical section will coincide with the maximum elevation of the separation surface. This is a zone of curvilinear flow, for which, for a given specific energy, the discharge is not necessarily the same as for parallel flow. Equation 1 applies only to rectilinear motion, and may not be used otherwise.

If, on the other hand, the weir entrance is sufficiently well rounded to prevent separation, the control section is shifted downstream. If this weir is of great enough length, a central region of essentially parallel flow will form which is free from the curvilinear effects at the two ends. If the fluid were frictionless, the depth of flow would be critical everywhere in this region. Actually, an appreciable boundary layer is formed in which are concentrated the viscous shear losses which are almost entirely responsible for the slope of the total-head line. By defining the discharge-displacement thickness of this boundary layer as the distance to which the boundary would have to be displaced to satisfy the equation of continuity if the velocity in the boundary layer were taken equal to the uniform, potential velocity outside the layer, and using this displacement thickness as an effective correction to be applied to the computed critical depth referenced to the weir crest, it seems possible that the traditional approach to the treatment of flow over a broad-crested weir with rounded entrance could be reconciled with that which has actually been found to exist. However, largely due to instrumentation difficulties, few boundary-layer measurements have been made in water, so that little progress has been made in this direction.

These considerations, in the light of present knowledge, restrict the use of the broad-crested weir as a critical depth meter whereby the discharge may be determined as a function of a single depth measurement. It may be pointed out, however, that all of these factors influencing the location of the critical-depth section and the shape of the water-surface profile over the weir are functions of weir geometry, weir roughness, and head on the weir. These parameters, likewise, control the head-discharge relation of the weir. Lacking a generalized method to permit the location and evaluation of the critical-flow depth on the weir, a functional form of the discharge coefficient must be sought that is based upon a combination of these variables into significant dimensionless ratios which adequately describe the pattern of flow. This is the method to be used here.

## DIMENSIONAL ANALYSIS

The following variables are sufficient to describe the flow characteristics of a level, broad-crested, nonsubmerged weir having vertical upstream and downstream faces and located in a long, smooth, horizontal, rectangular channel. In functional notation,

$$f(h \text{ or } p, V, \gamma, \rho, \mu, P, B, L, k, \tau) = 0. \quad (2)$$

The dimensions listed here are shown in figure 1. All symbols used are defined at the beginning of the report (facing p. 1).

There are 3 independent fundamental dimensions and 10 physical quantities involved in equation 2. By choosing  $h$ ,  $V$ , and  $\gamma$  as repeating variables, and combining these in succession with the remaining quantities, seven dimensionless ratios may be formed. Equation 2 thus becomes

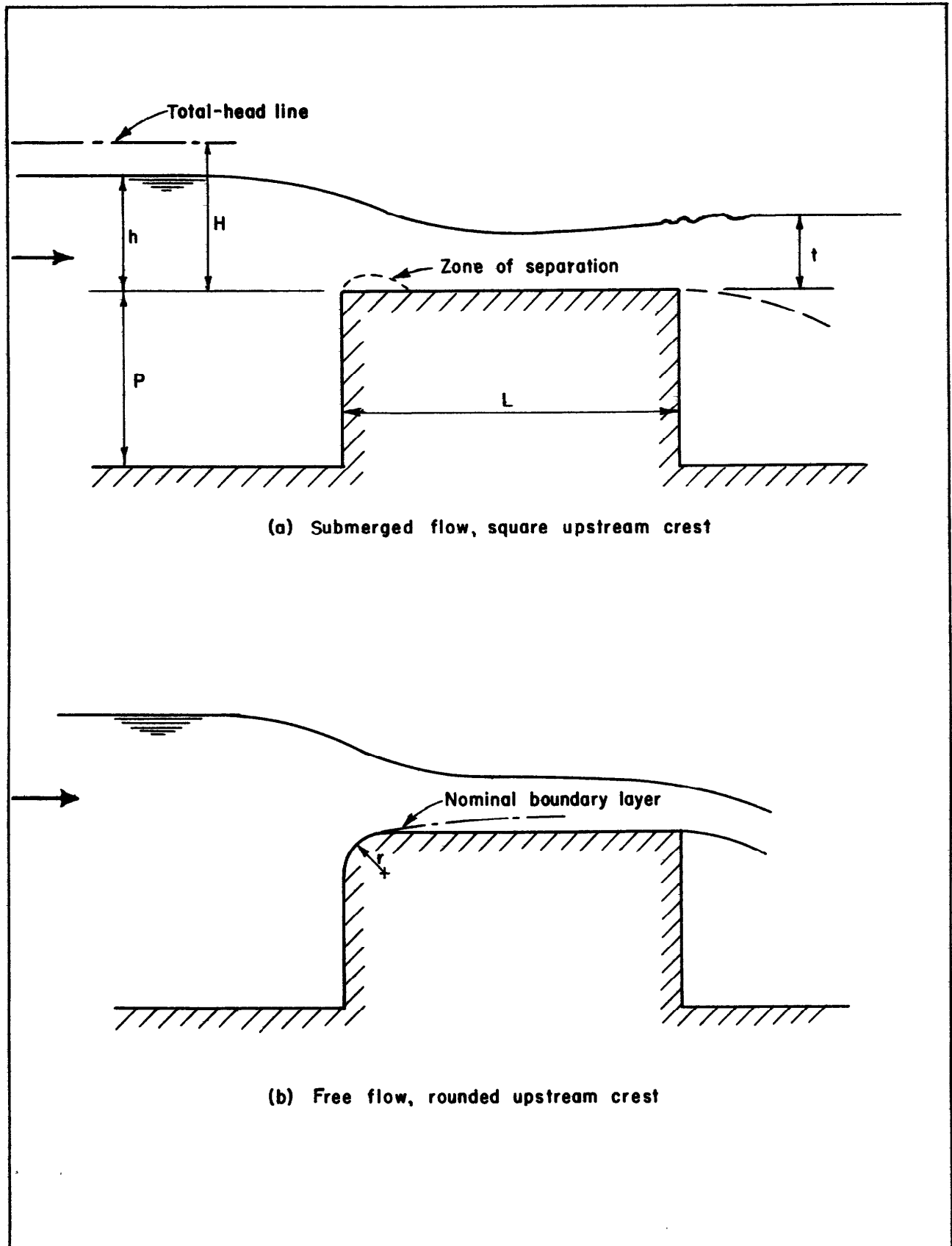


Figure 1. --Definition sketches of broad-crested weirs with vertical faces and horizontal crest.

$$f\left(\frac{V}{\sqrt{g\lambda}}, \frac{VH\rho}{\mu}, \frac{\lambda}{P}, \frac{\lambda}{B}, \frac{\lambda}{L}, \frac{\lambda}{k}, \frac{r}{\lambda}\right) = 0. \quad (3)$$

It will be observed that the first of these ratios in the left member of equation 3 has the form of a Froude number. Under the assumed flow conditions, however, the weir is a control structure, and the Froude number is not an independent variable; that is to say,  $V$  and  $\lambda$  cannot be varied independently of each other. For this reason, this characteristic number is best described as a coefficient of discharge and rewritten in the form  $C = Q/\{b\sqrt{g}\lambda^{3/2}\}$ .

The second ratio is recognized as the Reynolds number. Rearranging equation 3,

$$C = f\left(R, \frac{\lambda}{P}, \frac{\lambda}{B}, \frac{\lambda}{L}, \frac{\lambda}{k}, \frac{r}{\lambda}\right). \quad (4)$$

If, in the original array of variables, the surface tension of the fluid had been included as one of the variables influencing the flow pattern, the Weber number would have been produced as an additional dimensionless ratio. Except when the head is very small, the effect of surface tension is negligible and has hence been omitted from consideration altogether.

Thus, in equation 4, the coefficient of discharge is shown as a function of the Reynolds number and a number of independent length ratios involving the head and the physical dimensions of the weir. An explicit relation between the discharge coefficient and these variables is, of course, not known.

In the following sections of this report, the effect of each of these combinations of dimensionless variables upon the discharge coefficient will be investigated to the extent that it is possible with the data available.

#### EXTERNAL FLOW PATTERN

It will be helpful, before proceeding to an analysis of the variation of the coefficient of discharge as outlined in the preceding section, to consider some aspects of the external flow pattern of the broad-crested weir as evidenced by measured water-surface profiles. For this purpose, data by Prentice (1935) and Woodburn (1932) that represent two basic weir forms have been utilized. Sufficient generality is provided by these data to illustrate several significant points.

First, in figure 2A, the water-surface profile for flow over a level, broad-crested weir with vertical upstream and downstream faces is shown. The approach channel is rectangular and horizontal. The weir breadth is the same as the channel width. The weir surfaces are of planed wood or smooth concrete. The downstream nappe is fully aerated, and the weir entrance is square. The profile for the second weir form is shown in figure 2B. This weir is similar in all respects to that of figure 2A, except that the entrance is rounded.

These profiles have been made dimensionless by dividing both the depth of flow over the weir crest and the distance from the beginning of the weir by the piezometric head,  $\lambda$ , on the crest. The righthand ends of these curves represent the dimensionless flow depth at the downstream weir brink.

With the exception of two curves (those for an  $\lambda/L$  ratio of 0.40 and 0.073) the profiles for the weir with the square entrance (fig. 2A) exhibit strikingly similar configuration characteristics. In the accelerated-flow zone in the proximity of the entrance, the ratio

of depth to head decreases rapidly, its magnitude varying somewhat with the value of  $\lambda/P$ . Separation occurs at the sharp entrance to the crest, and the control section lies in the body of fluid above this separation zone. The flow becomes supercritical beyond this point. After passing through this crest zone, the flow begins to decelerate slightly, due to boundary resistance and to some expansion and consequent diffusion downstream from the separation zone. This deceleration is manifest in a slowly rising water-surface profile over the approximately parallel-flow region of the weir crest. Some distance downstream from the weir entrance, the profiles tend to superimpose, and the  $\lambda/P$  effect is no longer distinguishable.

If the weir crest is sufficiently long, the depth must eventually again approach the critical on the weir crest as the flow continues to decelerate with increased distance from the entrance. At this critical value, the specific head is the minimum at which this rate of flow is physically possible. A further energy loss, of necessity, causes an adjustment of depth and leads to the formation of a standing-wave pattern typical of flow at or near critical depth. This standing-wave configuration first appears when the weir length is roughly 12.5 times as great as the head on the weir, or at an  $\lambda/L$  ratio of about 0.080. All profiles for smaller ratios (not shown) of head to length show similar standing-wave characteristics.

If, on the contrary, the weir crest is relatively short and the head is large, the flow over the weir will be entirely curvilinear. In the upstream crest zone, this profile is somewhat lower vertically than that for the weir of great enough length to permit a zone of approximately parallel flow to form. This curvilinear profile appears when the  $\lambda/L$  ratio becomes greater than about 0.40. This bounding figure is, of course, not precise, but varies to some extent with the ratio of  $\lambda$  to  $P$ . Curves for  $\lambda/L$  values greater than 0.40 are not shown on figure 2A. It is evident, however, that as  $\lambda/L$  becomes larger, the water-surface profile must approach that of the upper water surface for a thin-plate sharp-crested weir.

Thus, broad-crested weirs may be divided into three groups with respect to the flow profile: short weir--entirely curvilinear flow; normal weir--curvilinear flow zones at the beginning and at the end of the weir crest, with a central zone of essentially parallel flow; and long weir--flow with a standing-wave pattern on the crest of the weir.

Approximate limits for these weirs, in terms of the  $\lambda/L$  ratio, have already been suggested. The weir is short if  $\lambda/L$  is larger than about 0.40, and is long if  $\lambda/L$  is less than about 0.08. Between these limits, the weir is normal. For the purpose of this report only the general limits are of importance.

It was suggested earlier that the flow is critical at a point near the downstream end of the weir at the transition between a normal and a long weir. It may be pointed out, as evidence of this, that the depth of flow at the downstream brink with respect to the weir head is remarkably constant. This depth for all the profiles of figure 2A at the brink is about  $0.43\lambda$ . The ratio of the brink depth to critical-flow depth for the free overfall has been fairly well established by Rouse (1936) as 0.715. Then, in terms of  $\lambda$ , the critical depth on the crest of the weir is  $0.43\lambda / 0.715 = 0.60\lambda$ , which is in good agreement with the maximum depth approached by the profiles of figure 2A near the downstream end of the weir for  $\lambda/L$  ratios near 0.08.

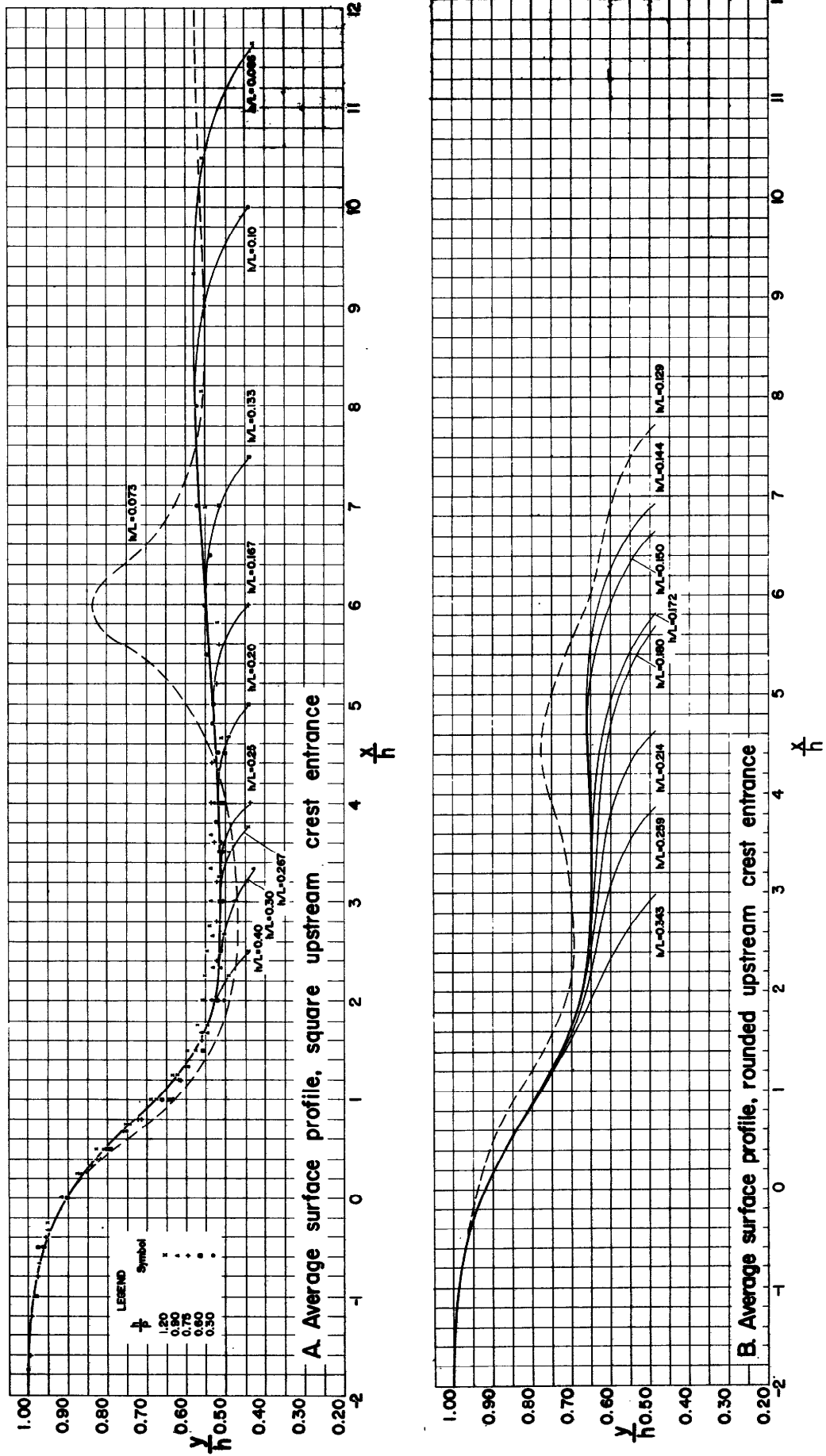


Figure 2.--Dimensionless water-surface profiles for broad-crested weirs with vertical faces and horizontal crest. (Data from Prentice, 1935, and Woodburn, 1932.)



The effect on the water-surface profile of rounding the weir entrance may be obtained from a comparison of figures 2A and 2B. The profiles for the two weir forms have the same general shape. The profiles for the weir of figure 2B, however, are displaced upward vertically. Further, the range of  $h/L$  for the normal weir of figure 2B is much smaller than its counterpart of figure 2A.

The energy losses in the separation zone just downstream from the beginning of the weir with the square upstream entrance may be estimated from these two figures. Assuming that the flow is critical at a point just upstream from the drawdown zone over the downstream crest exit for both weirs at the limit of the normal weir,  $y_c$  for the weir with the square entrance is about  $0.58h$  and for the weir with the rounded entrance is  $0.67h$ . The difference between these two depths represents the energy losses in the separation zone if it may be assumed that the resistance losses along the weir crests are approximately equal for both weirs, and if the reference head,  $h$ , may be considered to be roughly equal to the total head,  $H$ . This difference is  $0.09h$ .

#### DISCHARGE COEFFICIENT

##### Definition

In a preceding section, the coefficient of discharge was written in the form  $C = Q / (b\sqrt{g} h^{3/2})$ . It will be

more convenient to define this coefficient in terms of the total head,  $H$ , on the weir and to combine the term  $\sqrt{g}$  with the coefficient of discharge. Thus  $C = Q / (bH^{3/2})$ . The precepts of dimensional analysis are not violated by using  $H$  instead of  $h$ . Because of the dependency of  $V$  and  $h$ , the coefficient thus defined is functionally related to the same variables as the coefficient based upon the piezometric head,  $h$ .

#### Effect of Parameters Influencing the Coefficient

##### Weir Length

For the weir with a square entrance the dimensionless variable most important in fixing the value of the coefficient of discharge is the ratio  $h/L$ . The coefficient of discharge is shown as a function of this ratio in figure 3, which is defined from the data of several investigators. Here, each curve is identified by the name of the person responsible for the experimental work, and the source is given in the bibliography. The individual points through which these mean curves are drawn are not shown, but an idea of the magnitude of the scatter of these points about each curve may be obtained from a typical plot such as figure 7, for which the experimental data are shown.

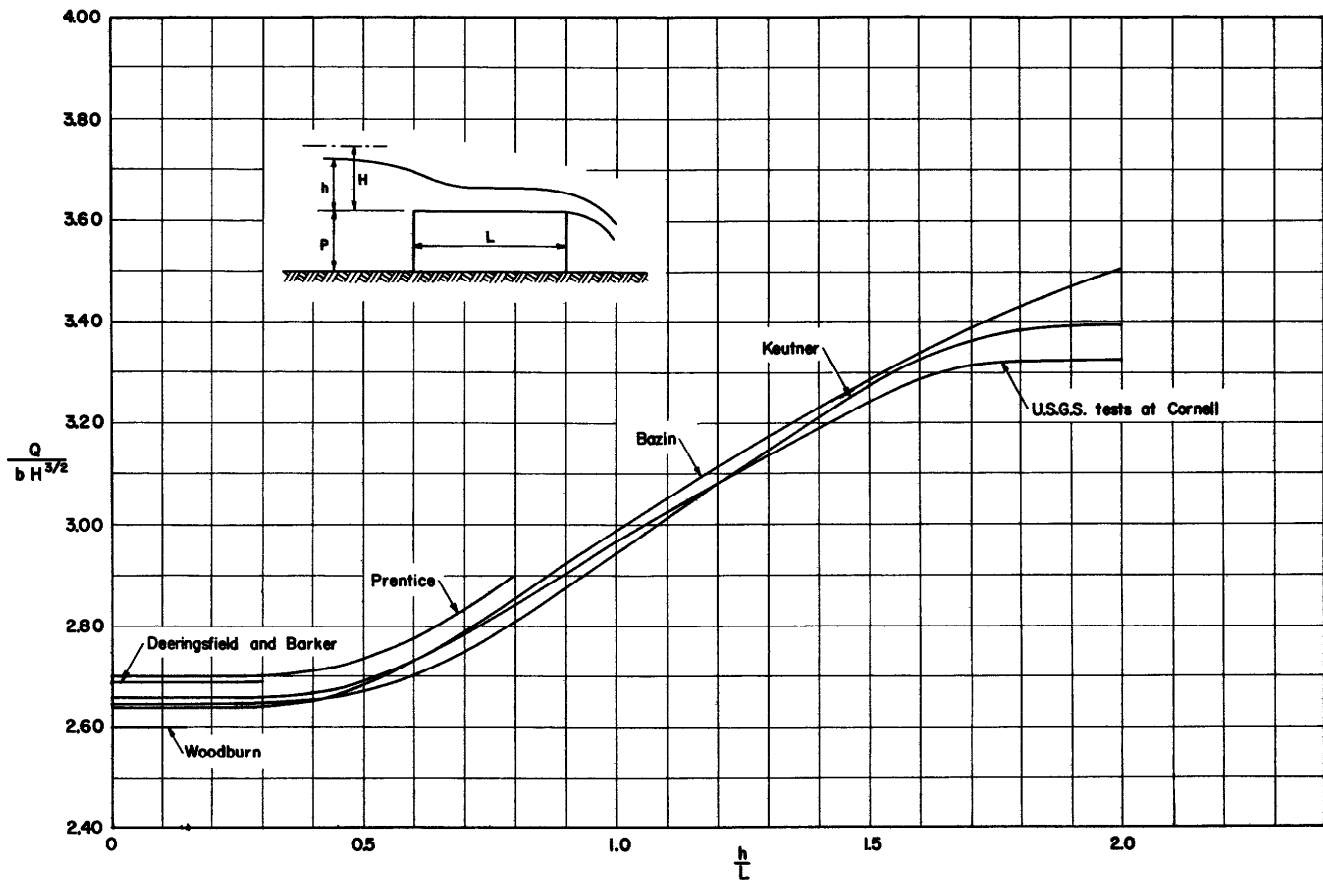


Figure 3. --Discharge coefficients for broad-crested weirs with vertical faces and horizontal crest, square entrance.

## Weir Height

In order to define the effect of a change in  $P$  upon the discharge coefficient, the deviations of the test points from the curves of figure 3 were plotted against the ratio  $h/P$ . No correlation between these deviations and the  $h/P$  ratio was found. It was therefore concluded that the effect of the  $h/P$  ratio is adequately compensated for by the use of the total head in computing the discharge coefficient. This is, in large part, the reason for substituting  $H$  for  $h$  in computing the discharge coefficient, and has been found to be advantageous even though the selection of a discharge coefficient from a chart where the coefficient is a function of the total head involves a solution requiring successive approximations.

The normal weir profiles (fig. 2A) show almost complete geometric similarity, except for some slight variation due to approach velocity. This geometrical similitude suggests that the discharge coefficient should then be very nearly constant in the range of  $h/L$  for the normal weir. This appears even more reasonable when one considers that the control section is just downstream from the entrance and over the separation zone, and that, because of this, the weir length does not affect the discharge. The lack of effect of  $h/P$  on the weir coefficient may perhaps be explained by the fact that the separation profile, as well as the surface profile, is affected by this variable, and that a compensation in the flow area at the critical section is obtained. These remarks, for less reason, have also been extended to the long

weir. It is conceivable, of course, that the weir could be long enough, or that the crest could be roughened to such an extent, so that the upstream channel control could be submerged by the downstream channel control. This possibility has not been considered.

In any event, the discharge coefficients for the long and the normal weir are shown as having a constant value in figure 3.

## Nappe Form

The literature contains many references to the importance of the nappe form in influencing the discharge coefficient. Given a nonaerated, nonsubmerged broad-crested weir, the nappe may assume any of the following forms, depending upon the head. These four forms are listed in their order of occurrence as the discharge increases.

1. Adherent to the downstream face of the weir.
2. "Depressed"; that is, some of the air under the nappe is entrained by the moving fluid and replaced by water, leaving the remaining air at less than atmospheric pressure.
3. "Wetted underneath"; all the air underneath the nappe is entrained and replaced by water, and the space formerly occupied by air is filled with eddying fluid.

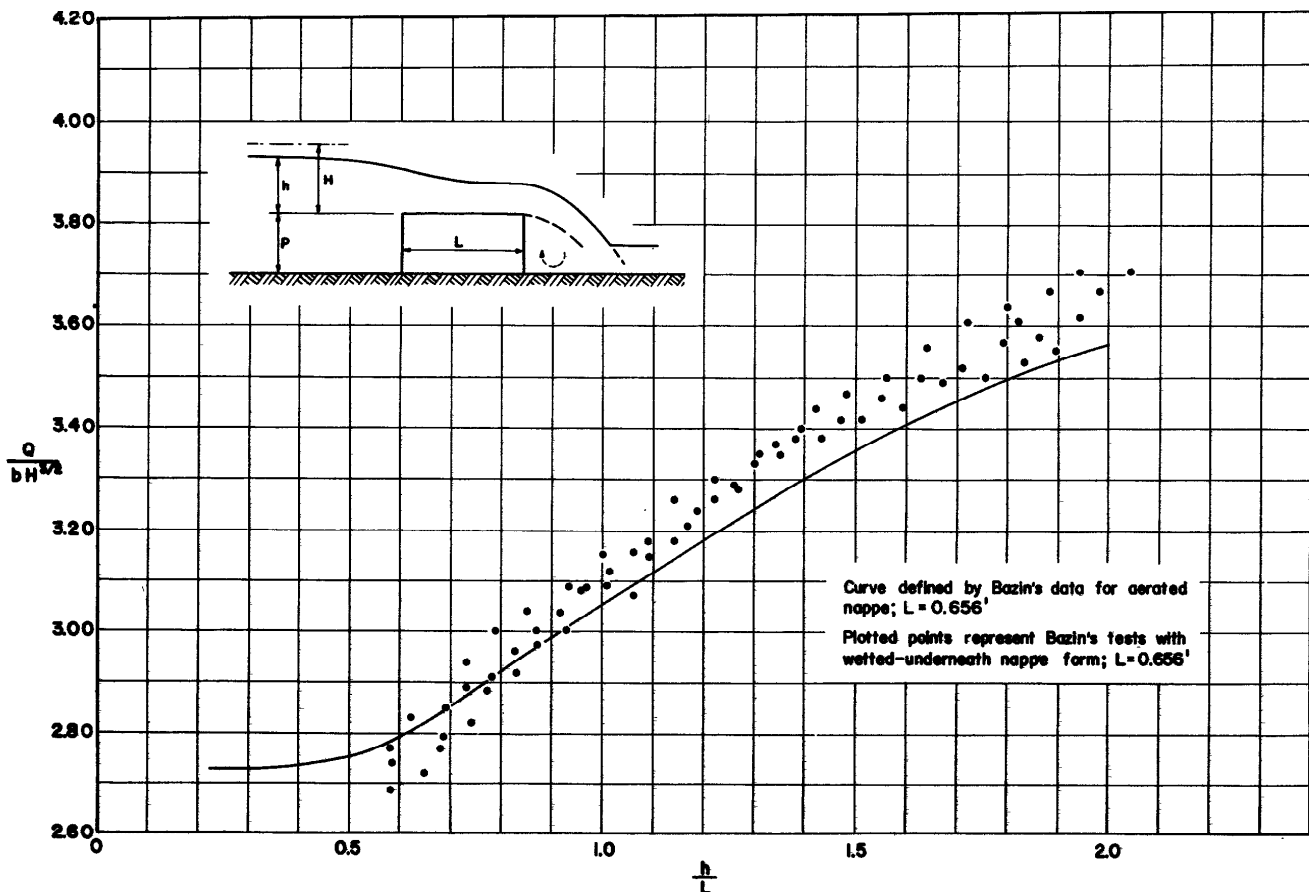


Figure 4. -- Effect of the wetted-underneath nappe form on the discharge coefficient.

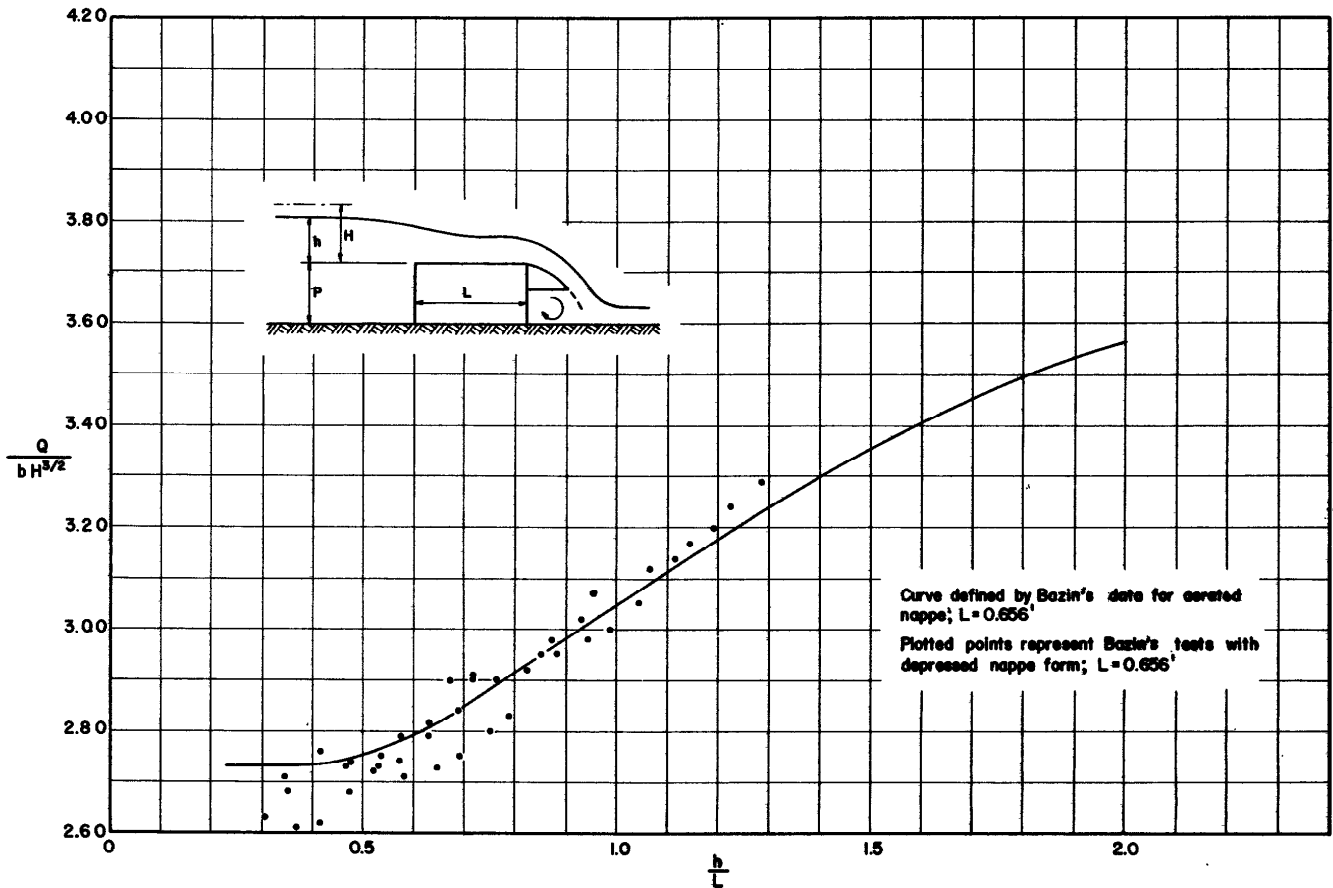


Figure 5. --Effect of the depressed nappe form on the discharge coefficient.

4. Free altogether of the flat crest of the weir and in contact with the weir only at the upstream face.

These nappes were named by Bazin (1896), who was among the first to investigate their effect on the discharge over the weir. The adhering nappe is usually of negligible importance and occurs only when the head is extremely low. The point at which one nappe form disappears and the next appears is somewhat indeterminate. These limits also change according to whether the discharge is increasing or decreasing, and are dependent upon the shape of the weir itself.

Complete data for the establishment of these transition ranges does not exist. The data of Bazin does, however, enable a comparison to be made between the coefficient of discharge for an aerated nappe and the coefficients for the wetted-underneath and depressed nappes, as shown in figures 4 and 5, respectively. In these figures, the plotted data represent the coefficient of discharge for these nappe forms, and the curves represent the coefficient of discharge for weirs with aerated nappes. These tests were made on level broad-crested weirs with vertical upstream and downstream faces. Apparently, from these figures, the overall change in the discharge coefficient due to a change from the aerated to the depressed or wetted-underneath nappe forms is on the order of 1 or 2 percent. This is almost inconsiderable for any exact very precise discharge determinations.

The point at which the nappe becomes detached at the upstream crest entrance and springs clear of the

weir crest varies somewhat, depending upon the completeness of aeration of the space beneath the downstream nappe, the  $h/P$  ratio, and upon the sharpness of the entrance; it usually occurs suddenly. The tests made by Bazin indicate that it may occur at an  $h/L$  as low as 1.5, or as high as 2.0, for aerated weirs. Once the nappe springs clear of a broad-crested weir, it is usual to assume that the weir acts as a thin-plate, sharp-crested weir. In figure 6, the tests made by Bazin on level broad-crested weirs with vertical faces, square entrances, and detached nappes are compared with the curve defined by Bazin's data for thin-plate, sharp-crested weirs. It will be noted that the agreement of the plotted points with the curve is somewhat less than ideal; this may possibly be attributed to the lack of true sharpness of the entrance to the broad-crested weir.

#### Reynolds Number

A definite variation in the coefficient of discharge with scale ratio is to be expected. This so-called scale effect is the result of the action of the forces due to the viscosity of the fluid. The Reynolds number is used to describe the relative importance of the viscous forces; the larger the Reynolds number, the less important the influence of viscosity upon the flow pattern. The Reynolds number of equation 3, for a given fluid, is proportional to  $\lambda^{3/2}$ , or to the discharge per foot of width of the weir. From this, it is obvious that the Reynolds numbers of model and prototype can be equal only at the same scale. It is thus usually impracticable to satisfy the Reynolds law

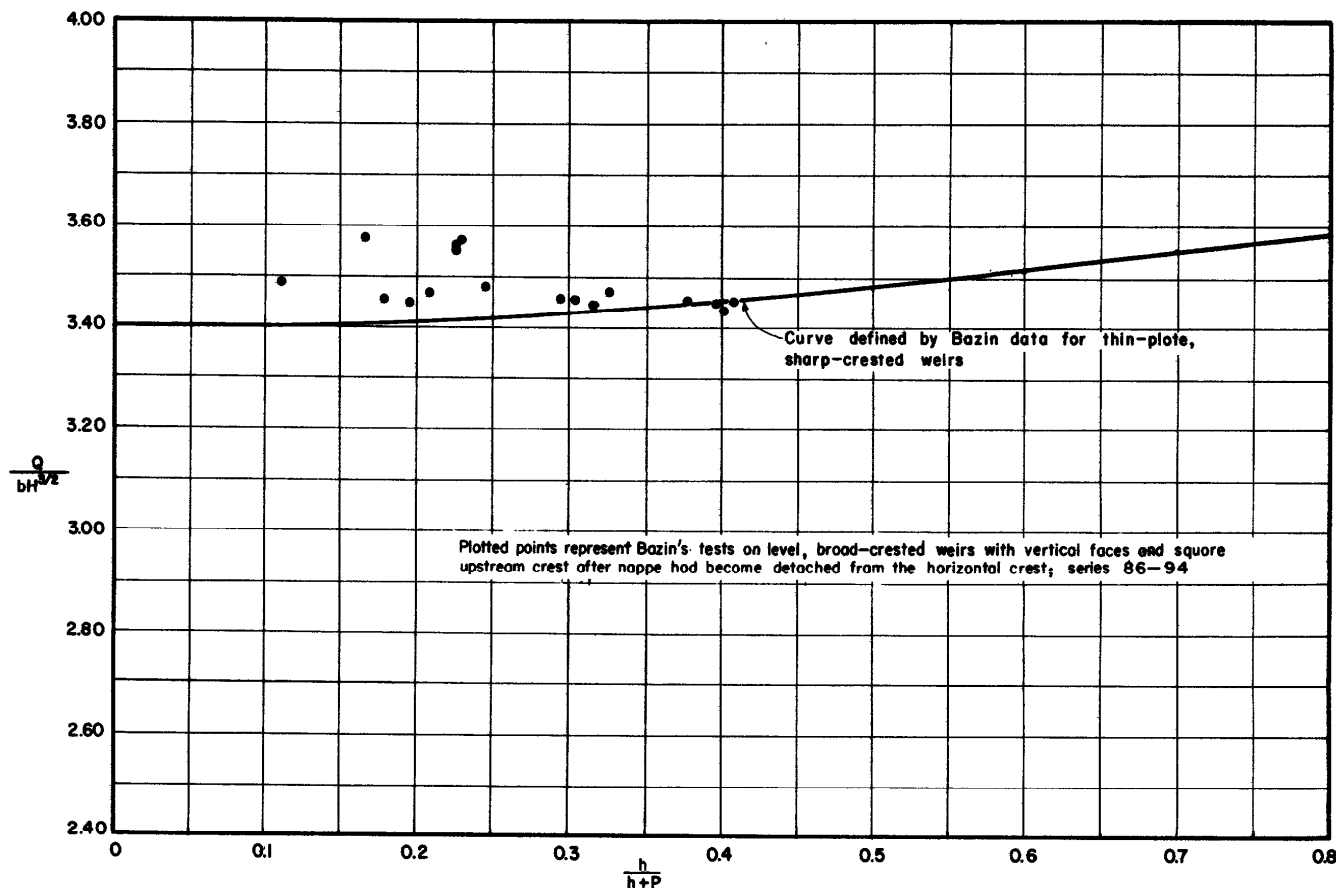


Figure 6. -- Effect of the detached nappe form on the discharge coefficient.

completely. Generally, however, it is possible to obtain Reynolds numbers in the laboratory sufficiently high to include the range in which the effects of fluid viscosity may be ignored.

Two noteworthy studies have been made to determine the effect of scale on the discharge coefficient. These experiments were made on nappe-shaped weirs. The first, reported by Eisner (1933), describes tests made on models at scales of 1:70, 1:35, 1:17.5, 1:8.75, and 1:4.375. An increase in discharge coefficients was noted with an increase in model scale; this effect was attributed by Eisner to the relative roughness of the boundary surface--absolute roughness being the same in each of the several models.

From measurements made on geometrically similar models of the nappe-shaped Pickwick Landing spillway at scales of 1:200, 1:100, and 1:500, Kirkpatrick (1955) concluded that the scale of the model does not affect the relation between head and discharge coefficient. He found no consistent deviation of the discharge coefficient at the three scales and therefore attributed the small variations to experimental error.

For the broad-crested weir, Bazin's experiments furnish sufficient data to determine the Reynolds number effect qualitatively. In figure 7 are plotted the results of Bazin's measurements on weirs of rectangular shape and square upstream entrances, and at various scale ratios. For the lowermost curve the scale is 8 times as large as that for the uppermost curve, for the next curve 4 times as large, and for the third curve

twice as large. The scale of  $P$  is not considered in these tests as it has been shown to have no effect on the discharge coefficient. For Bazin's tests the coefficient of discharge decreases with increasing scale, or with increasing Reynolds number.

With a very few exceptions, these plotted points represent tests on short weirs. The heads for the uppermost curve are very small, so that the deviation of these points may perhaps be ascribed primarily to effects of surface tension. The slight variation between the remaining three curves is due to some differences in energy required to maintain the eddy motion in the separation zone as the weir scale increases. For the rounded-entrance weir, this trend is probably reversed; that is, it would be expected that the coefficient will increase with increased scale, and for the same reasons that the Eisner coefficients were found to increase.

Because the U. S. Geological Survey tests at Cornell (see fig. 3), made at a much greater scale than Bazin's tests, agree fairly well with the lowermost of Bazin's curves on figure 7, it is assumed that for weirs at least as large as Bazin's largest, the Reynolds number is large enough so that the effects of fluid viscosity may be ignored. Most structures found in the field are of much greater size. For these, the the lowermost curve of figure 7 should be used to select a discharge coefficient.

#### Rounded Weir Entrance

The effect of rounding the upstream entrance to the weir is to increase the discharge coefficient by

removing the cause of the flow separation at the crest entrance, which is the primary source of energy loss. This variation in the discharge coefficient has been shown to be a function of  $r/h$  in equation 2, but sufficient data to completely define the function do not exist. Woodburn ran a series of tests in which he systematically varied the upstream crest-entrance radius of rounding from 0 to 8 inches in 2-inch increments. The discharge coefficients for the 2-, 4-, 6-, and 8-inch roundings ( $r/h > 0.15$ ) superpose and are about 9 percent greater than the corresponding coefficients for the square entrance ( $r/h = 0$ ).

This data may be interpreted by analogy with similar data for the contracted opening. Kindsvater and Carter (1955) demonstrated that the discharge coefficient for contracted openings increased almost linearly with the values for  $r/b$  from  $r/b = 0$  to  $r/b = 0.14$ ; the coefficient remained constant after  $r/b$  exceeded 0.14. A similar variation in the coefficient of discharge for orifices has been demonstrated in the literature.

For the lack of a more exact procedure, it is suggested that a discharge coefficient be chosen for the rounded-entrance weir equal to 1.09 times the coefficient for the square entrance if the value of  $r/h$  is greater than 0.14. For intermediate values of  $r/h$  the adjustment may be interpolated between the extremes of unity and 1.09.

Boundary Roughness

One of the most troublesome aspects of model testing is the difficulty involved in duplicating in the model

the surface resistance of the prototype. For a given test structure having a given boundary roughness, the energy losses due to boundary resistance are a function of a characteristic Reynolds number and the relative roughness. As the scale is decreased, the relative roughness increases, and the boundary shear force thus becomes disproportionately large if the boundary surfaces are of the same material for the various scales.

The relative roughness is usually described by relating the mean height of the boundary projections above the nominal surface level to some significant length. Here, the ratio  $h/k$  is used, where  $k$  is the mean roughness height. Thus, only if the relative roughness and the Reynolds number are equal in model and prototype is there assurance that the relative effect of boundary resistance is the same at both scales. It is generally impractical, if not impossible, to arrange equal values of either  $R$  or  $h/k$ . Requirements of similitude are compromised by either ignoring the difference in relative roughness or by extension to the scale of the prototype by the use of some method based on experience.

Here, again, definitive data for a determination of the effect of boundary roughness are not at hand. Unless the model is extremely small, it is usual to apply the results from it to much larger scale structures. In general, if the influence of boundary roughness is considered separate from other effects, the discharge coefficient should increase slightly as the scale of the model increases.

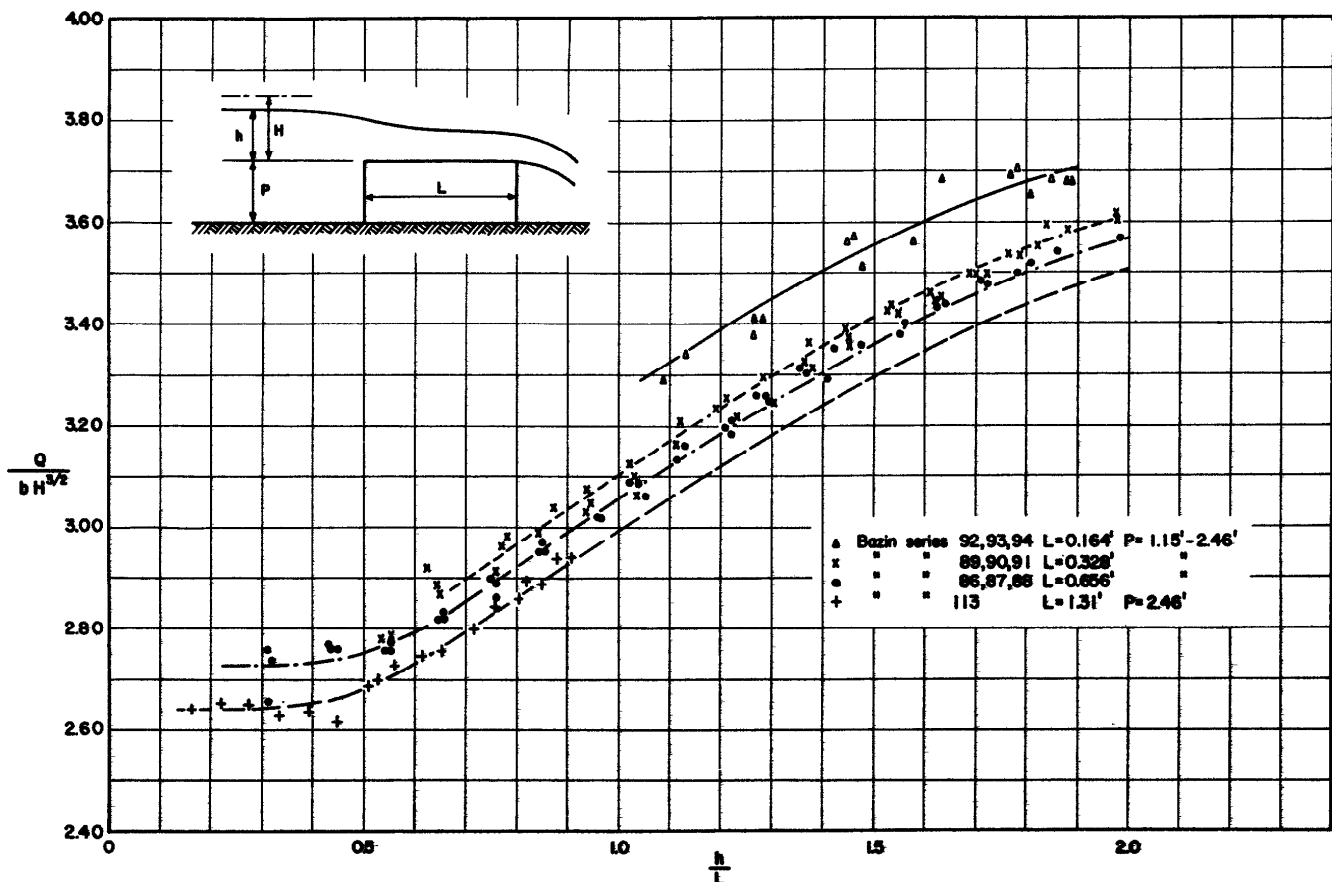


Figure 7. --Variation of the discharge coefficient with scale of weir. (Data from Bazin, 1896.)

Shape Ratio

The remaining variable of equation 3,  $h/B$ , may be interpreted as a shape parameter. It was not found to be significant in the range for which test data are available.

Sloping Upstream and Downstream Faces

In figures 8-11, the discharge coefficient for level, broad-crested weirs having various combinations of upstream- and downstream-face slope is shown. The test data are from the experiments of Bazin.

In each of these figures, the upstream-face slope is constant. Thus, figure 8 represents the discharge co-

efficients for weirs having a vertical upstream-face slope, figure 9 the coefficients for weirs with an upstream-face slope of 1/2:1, figure 10 the discharge coefficient for a weir with an upstream-face slope of 1:1, and figure 11 the coefficient for a weir with an upstream-face slope of 2:1. The families of curves shown on each of these figures represent the discharge coefficients for various downstream-face slopes. Interpolated curves are shown as dashed lines.

Submergence

Submerged weirs (fig. 1A) are beyond the scope of this report. Generally, it appears that the nonsubmerged-weir coefficients may be applied to weirs for which the ratio  $t/h$  is equal to or less than 0.85.

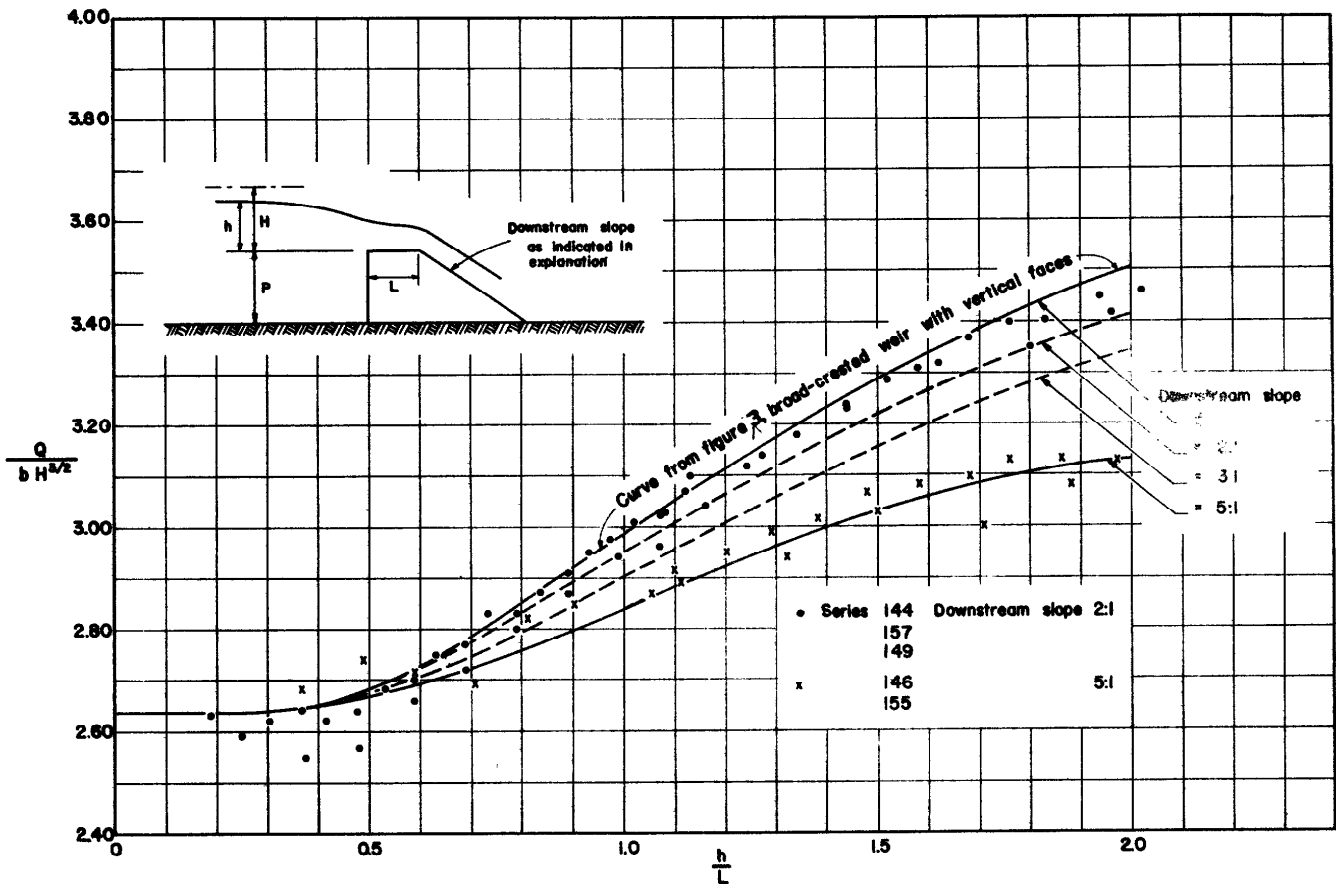


Figure 8. --Discharge coefficients for broad-crested weirs with vertical upstream face. (Data from Bazin, 1896.)

DISCHARGE CHARACTERISTICS OF BROAD-CRESTED WEIRS

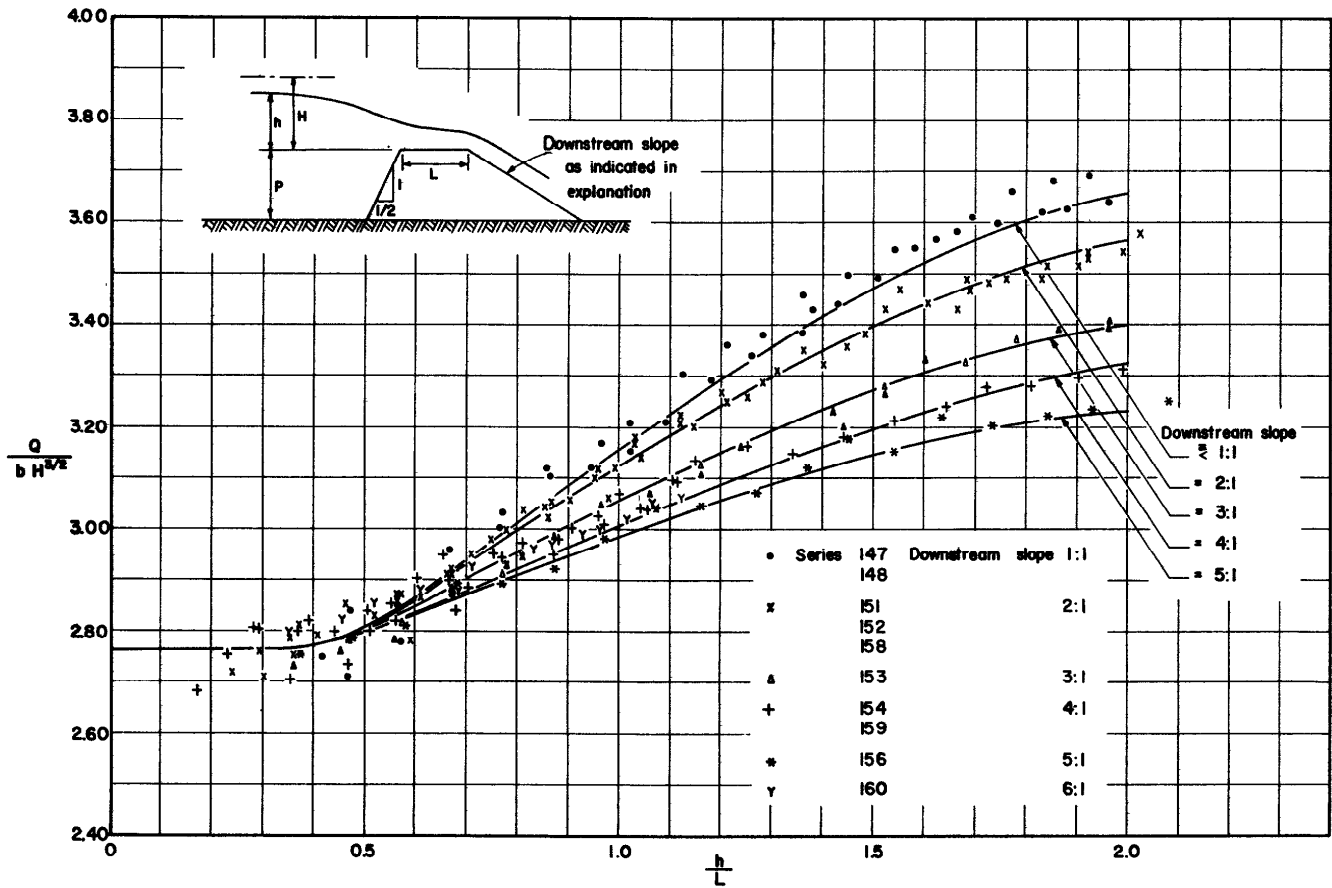


Figure 9. --Discharge coefficients for broad-crested weirs with upstream-face slope of 1/2:1. (Data from Bazin, 1896.)

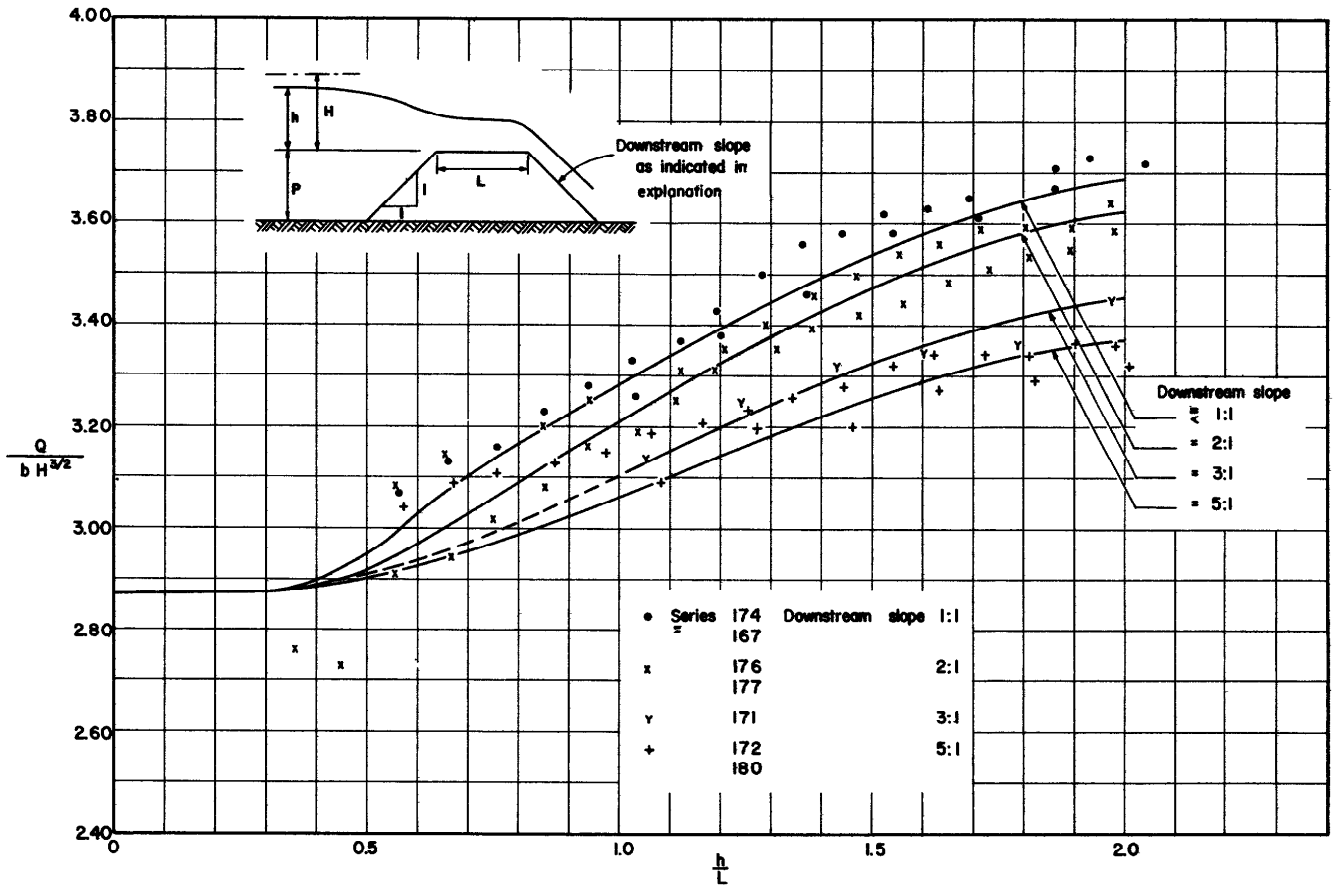


Figure 10. --Discharge coefficients for broad-crested weirs with upstream-face slope of 1:1. (Data from Bazin, 1896.)



DISCHARGE CHARACTERISTICS OF BROAD-CRESTED WEIRS

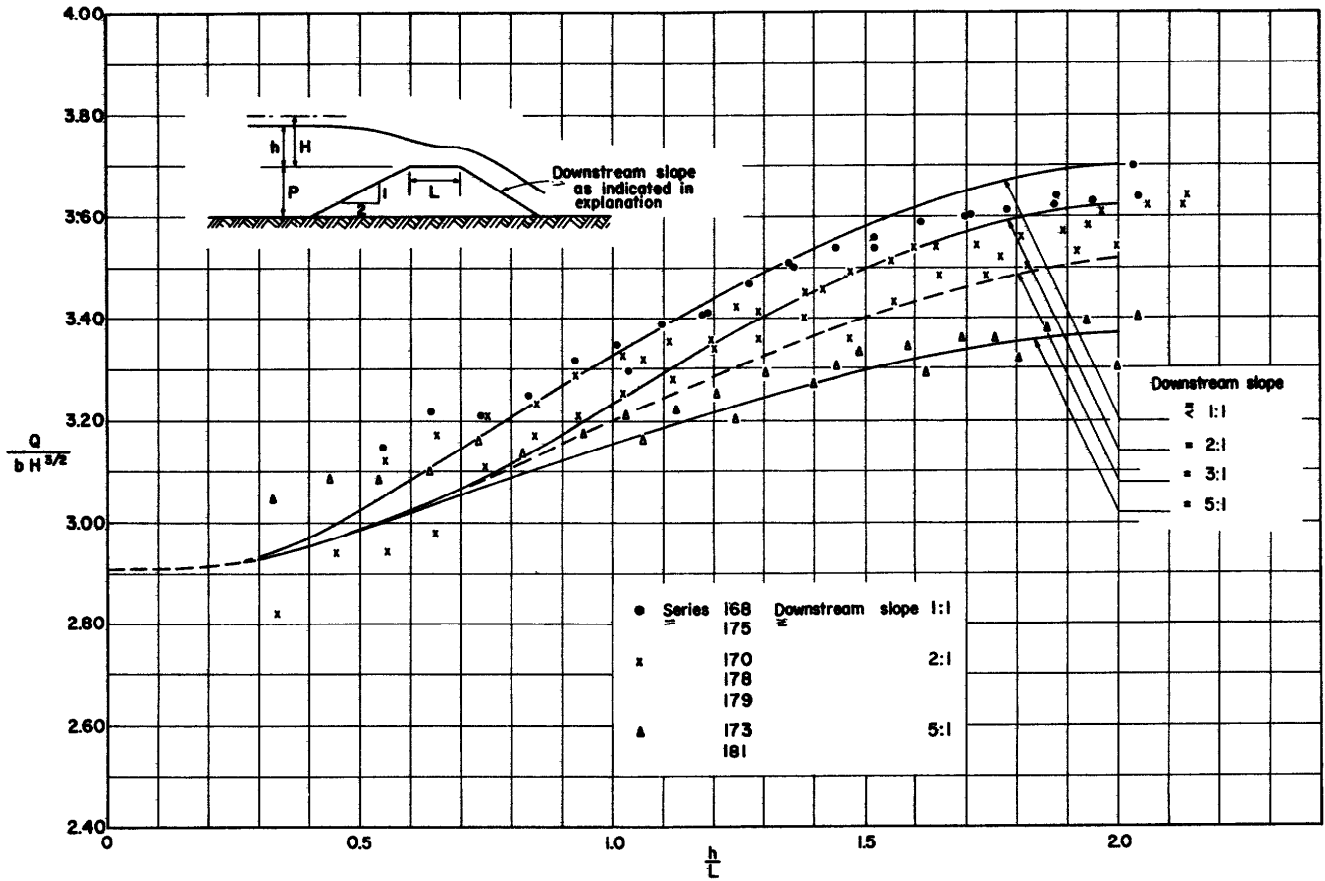


Figure 11. --Discharge coefficients for broad-crested weirs with upstream-face slope of 2:1. (Data from Bazin, 1896.)

Published Reports

- Bazin, M. H., 1896, Expériences nouvelles sur l'écoulement en déversoir: Annales des Ponts et Chaussées, v. 7, ser. 7.
- Böss, Paul, 1929, Berechnung der Abflussmengen und der Wasserspiegellage bei Abstürzen und Schwellen unter besonderer Berücksichtigung der dabei auftretenden Zusatzspannungen: Wasserkraft und Wasserwirtschaft, nos. 2-3, p. 13-14, 28-33.
- Doeringsfeld, H. A., and Barker, C. L., 1941, Pressure-momentum theory applied to the broad-crested weir: Am. Soc. Civil Engineers Trans., v. 106, p. 934.
- Eisner, Franz, 1933, Überfallversuche in verschiedener Modellgröße: Mitt. Preussischen Versuchsamt, Wasserbau und Schiffbau [Berlin], no. 11.
- Forchheimer, Philipp, 1930, Hydraulik: B. G. Teubner, Leipzig and Berlin, p. 373-410.
- Hailer, Rudolf, 1929, Fehlerquellen bei der Überfallmessung: Mitt. Hydraul. Inst. Techn. Hochschule Munschen, no. 3.
- Horton, R. E., 1907, Weir experiments, coefficients, and formulas: U.S. Geol. Survey Water-Supply Paper 200.
- Ippen, A. T., 1950, in Rouse, Hunter (ed.), Engineering hydraulics: New York, John Wiley and Sons, Inc., p. 526-27.
- Keutner, Chr., 1934, Strömungsvorgänge an breitkrönigen Wehrkörpern und an Einlaufbauwerkern: Der Bauingenieur, v. 15, p. 366.
- Kindsvater, C. E., and Carter, R. W., 1955, Tranquil flow through open-channel constrictions: Am. Soc. Civil Engineers Trans., v. 120, p. 955.
- King, H. W., 1954, Handbook of hydraulics: New York, McGraw-Hill Book Co., 4th ed., p. 5-1 to 5-15.
- Kirkpatrick, K. W., 1955, Discharge coefficient for spillways at TVA dams: Am. Soc. Civil Engineers Separate 626.
- Moore, W. L., 1943, Energy loss at the base of a free overfall: Am. Soc. Civil Engineers Trans., v. 109, p. 1343.
- Musterle, Th., 1930, Abflussberechnungen bei Wehren mit breiter Krone mit Hilfe des Impulssatzes: Die Wasserwirtschaft, no. 21.
- Rouse, Hunter, 1933, Verteilung der Hydraulischen Energie bei einem lotrechten Absturz: Munich and Berlin, R. Oldenburg.
- 1936, Discharge characteristics of the free overfall: Civil Eng. v. 6, no. 4, p. 257.
- United States Bureau of Reclamation, 1948, Studies of crests for overfall dams: Boulder Canyon Proj., Part 6, Bull. 3.
- Woodburn, J. G., 1932, Tests of broad-crested weirs: Am. Soc. Civil Engineers Trans., v. 96, p. 387.
- Yarnell, D. L., 1930, Flow of water over railway and highway embankments: Public Roads, v. 2, April, p. 30.

Unpublished Reports

- Delleur, J. W., 1955, Boundary layer development in open channels: Columbia Univ., Civil Eng. Dept., Ph. D. thesis.
- Guernesey, Robert, Jr., 1940, The boundary layer in a broad-crested weir: Columbia Univ., Civil Eng. Dept., M. S. thesis.
- Krimgold, D. D., and Perko, F. L., 1936, Investigation of the laws of similitude as applied to flow of water over broad-crested weirs: Univ. of Calif., Civil Eng. Dept., B. S. thesis.
- Joe, A. K., and Thomson, G. C., 1937, A report on the similarity of models of broad-crested weirs: Univ. of Calif., Civil Eng. Dept., B. S. thesis.
- Prentice, T. H., 1935, Hydraulics of the broad-crested weir: Columbia Univ., Civil Eng. Dept., M. S. thesis.
- Schmidt, M. O., 1941, Tests of a flat-crested weir: Univ. of Wisconsin, M. S. thesis.
- Sigurdsson, Gunnar, 1955, Discharge characteristics of an embankment-shaped weir: Georgia Inst. of Technology, Civil Eng. Dept., M. S. thesis.
- Sullivan, A. B., and Davis, J. W., 1936, A report on discharge coefficients for broad-crested weirs: Univ. of Calif., Civil Eng. Dept., B. S. thesis.



